

Multi-Channel Design for Iterative Learning Control

Yongqiang Ye and Danwei Wang

Abstract— In this paper, a *multi-channel* method is proposed for design of iterative learning control. This novel design method uses multiple channels to widen the learning frequency range that can be achieved by a single channel. The application of the multi-channel method to the anticipatory learning control design is analyzed in details. The design procedure and effectiveness of the multi-channel method are demonstrated via an example and simulations. Comparisons of the multi-channel learning control with the conventional single channel learning control highlight the application prospect of the multi-channel design method.

I. INTRODUCTION

Iterative learning control (ILC) develops controllers that are to perform a specific tracking command repeatedly, each time starting from the same initial condition [1]. It aims to reduce tracking error during the whole period of a process operation including the transient part using minimum knowledge of the system. This is accomplished by using the past experience(s) to improve the performance in the future operations. The input signal is updated based on the recorded data from previous trials to make the output converge to the desired output.

Since its emergence, ILC has received considerable attention. In the growing stage of ILC, researches focus on convergence issues. But in applications, the mathematically proved convergence of ILC does not guarantee reasonable transients during the learning process [12]. And it is the time to exhibit the usefulness and effectiveness of learning control through real-life examples, show that learning control does offer new concepts and new solutions. Therefore, in recent years, increasing efforts have been made on the design issues. Efforts in ILC design include using techniques like Linear Matrix Inequality (LMI) [4], H_∞ [2], μ -synthesis [16], Auto-Regressive Moving Average (ARMA) model approximation [17], and zero-phase filtering [12], [20].

In most ILC papers, the input update is acquired directly from the error information of the previous repetition(s). An alternative approach is that the frequency coefficients of the input update is firstly derived from the Discrete Fourier Transform (DFT) of the previous error, then the input update is achieved via Inverse Discrete Fourier Transform (IDFT) [9], [10], [15]. The later approach offers flexibility in dealing with individual harmonic components of the tracking error. If n harmonic components are considered, the learning control has n parallel learning compensators in the frequency domain. The *multi-channel* design method

proposed in this paper has a few, generally much less than n , learning compensators working simultaneously, and the input update still takes place in the time domain. This method bridges the existing two approaches. The multi-channel learning deals with the tracking error channel-wise ('channel' means a designated frequency band). In this paper, we will present the theoretical issue of the multi-channel method. Experimental results on a robot joint were reported in [24].

II. SINGLE CHANNEL ILC DESIGN

Consider a physical system modeled by a SISO continuous time invariant linear state space equation

$$\begin{cases} \dot{x}(t) = Ax(t) + Bu(t) + w(t) \\ y(t) = Cx(t) \end{cases} \quad (1)$$

where x is the n -dimensional state vector, u is the scalar input, y is the scalar output and w represents any deterministic disturbances that appear in every repetition. Laplace transform of the output for the j th repetition is

$$Y_j(s) = G_p(s)U_j(s) + C(sI - A)^{-1}x(0) + C(sI - A)^{-1}W(s) \quad (2)$$

where $G_p(s) = C(sI - A)^{-1}B$ is the input-output transfer function and $x(0)$ is the initial state position which is assumed to be the same for each repetition. The tracking error of the j th repetition is $E_j(s) = Y_d(s) - Y_j(s)$, where $Y_d(s)$ is the Laplace transform of a desired output $y_d(t)$ defined over a finite time operation interval $[0, T]$. Let the Laplace transform of the learning law be

$$U_j(s) = U_{j-1}(s) + k\Phi(s)E_{j-1}(s) \quad (3)$$

where k is the scalar learning gain and $\Phi(s)$ is the learning compensator in Laplace form (the DC gain of $\Phi(s)$ is supposed to be 1; if it is not 1, this value can be absorbed by k). Use (2) and (3) and we get

$$\begin{aligned} Y_j(s) - Y_{j-1}(s) &= G_p(s)[U_j(s) - U_{j-1}(s)] \\ &= kG_p(s)\Phi(s)E_{j-1}(s). \end{aligned}$$

Since

$$Y_j(s) - Y_{j-1}(s) = -[E_j(s) - E_{j-1}(s)],$$

we get

$$E_j(s) = [1 - kG_p(s)\Phi(s)]E_{j-1}(s). \quad (4)$$

$[1 - kG_p(s)\Phi(s)]$ can be viewed as a transfer function from the tracking error at repetition $(j-1)$ to the tracking error at repetition j . Similar to [3], [7], [8], [12], the condition for

The authors are with School of Electrical and Electronic Engineering, Nanyang Technological University, Singapore 639798 edwwang@ntu.edu.sg

the tracking error to decay monotonically every repetition for all frequencies is

$$|1 - kG_p(j\omega)\Phi(j\omega)| < 1. \quad (5)$$

Frequency domain convergence condition is a sufficient condition for convergence though learning control is finite time problem [2], [12]. In practice, it is difficult to make (5) satisfied for all frequencies. The frequency range where (5) holds is termed the *learnable frequency band (range)*. A cutoff is required to stop learning the error components with frequencies at which this condition is violated.

III. LEARNING CHANNEL-WISE

A. Multi-Channel ILC Structure

If the learnable frequency band of a single channel learning control is not wide enough, methods to extend the learnable frequency band are required. Longman and Wirkander use the self tuning method, switching the parameters of the learning compensator between repetitions and finding the best switch mode [14], [23]. The switch results in a much higher cutoff frequency [23]. Longman and Wirkander's idea can be generalized into switching the learning compensators, not just switching parameters. If we use learning compensator $\Phi_1(s)$ with learning gain k_1 for α trials, then switch to $\Phi_2(s)$ with learning gain k_2 for β trials, then repeat, the total error contraction rate is

$$|1 - k_1G_p(j\omega)\Phi_1(j\omega)|^\alpha |1 - k_2G_p(j\omega)\Phi_2(j\omega)|^\beta.$$

It is possible to find an optimal ratio of α/β that will keep the total error contraction rate less than one up to the highest frequency. And this frequency will be higher than the cutoff frequency of using $\Phi_1(s)$ with k_1 or $\Phi_2(s)$ with k_2 alone.

The multi-channel method proposed here also aims to use more learning compensators to cover a wider frequency band, but in a different direction. A new ILC structure with n channels is proposed in Fig. 1. The filter $F_i(s)$ defines the designated frequency band of the i th channel, k_i is the learning gain for the i th channel, and the i th learning compensator $\Phi_i(s)$ ensures convergence of the tracking error within the defined frequency band (suppose the DC gain of $\Phi_i(s)$ is 1; if it is not 1, this value can be absorbed by k_i). The tracking error is separated into n parts corresponding to the designated bands/channels. These separated error parts are learned simultaneously in corresponding channels. The individual learning control laws in the individual channels are

$$\begin{cases} U_{1,j}(s) = U_{1,j-1}(s) + k_1\Phi_1(s)F_1(s)E_{j-1}(s) \\ \quad \text{In Channel 1} \\ \vdots \\ U_{i,j}(s) = U_{i,j-1}(s) + k_i\Phi_i(s)F_i(s)E_{j-1}(s) \\ \quad \text{In Channel } i \\ \vdots \\ U_{n,j}(s) = U_{n,j-1}(s) + k_n\Phi_n(s)F_n(s)E_{j-1}(s) \\ \quad \text{In Channel } n \end{cases} \quad (6)$$

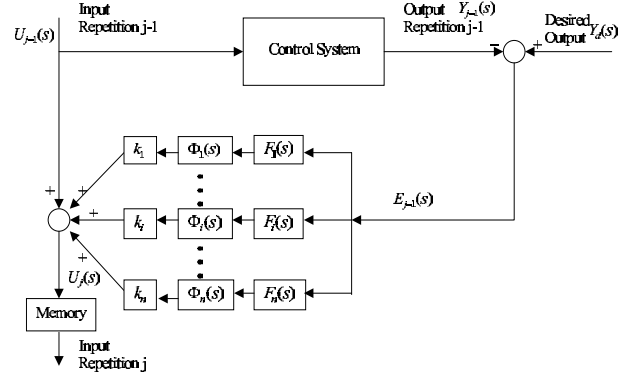


Fig. 1. Multi-channel learning control

Note that different learning gains can be used in different channels. For example, we can use a smaller learning gain in high frequency channels to decrease system sensitivity to random high frequency noises but still assure a reasonable learning speed. This is another benefit of the multi-channel method besides learnable band extension. The overall learning law is

$$\begin{aligned} U_j(s) &= \sum_{i=1}^n U_{i,j}(s) \\ &= \sum_{i=1}^n U_{i,j-1}(s) + \left(\sum_{i=1}^n k_i\Phi_i(s)F_i(s) \right) E_{j-1}(s) \\ &= U_{j-1}(s) + \left(\sum_{i=1}^n k_i\Phi_i(s)F_i(s) \right) E_{j-1}(s). \end{aligned} \quad (7)$$

Using (5) and (7), the error contraction condition for multi-channel learning control is

$$\left| 1 - G_p(j\omega) \left(\sum_{i=1}^n k_i\Phi_i(j\omega)F_i(j\omega) \right) \right| < 1. \quad (8)$$

The time domain version of (7) and (6) are

$$u_j(t) = \sum_{i=1}^n u_{i,j}(t) \quad (9)$$

with

$$\begin{cases} u_{1,j}(t) = u_{1,j-1}(t) + k_1L_1(e_{1,j-1}(t)) \\ \quad \text{In Channel 1} \\ \vdots \\ u_{i,j}(t) = u_{i,j-1}(t) + k_iL_i(e_{i,j-1}(t)) \\ \quad \text{In Channel } i \\ \vdots \\ u_{n,j}(t) = u_{n,j-1}(t) + k_nL_n(e_{n,j-1}(t)) \\ \quad \text{In Channel } n \end{cases} \quad (10)$$

where $L_i(\cdot)$ is channel i 's learning algorithm corresponding to $\Phi_i(s)$ and $e_{i,j-1}(t)$ is the result of passing error at repetition $j-1$, $e_{j-1}(t)$, through filter $F_i(s)$. It should be noted that the input update of the multi-channel learning control still takes place in the time domain which is different from the approaches in [9], [10], [15]. The total input update

is the sum of multiple learning control updates. In the time domain, Tayebi and Zaremba proposed gain-scheduling-based iterative learning controllers for continuous-time nonlinear systems described by a blended multiple model representation [19]. In [19], the learning gain changes according to the values of the validity functions depending on the operating point in the time domain, while in our approach, the learning compensator or parameter depends on frequency. The idea of using summational multiple functions to represent a blended model is the same in our multi-channel method and [19].

Remark 1 The price paid for the multi-channel method is that the multi-channel learning control has the computational burden of n learning controllers. For easy application, ILC design should use as few as possible channels to cover the required frequency band. First, a learning compensator is chosen with a substantially broad learnable band. If the learnable band meets the learning control specification, the design is completed and no multi-channel is needed. If the learnable band is not satisfactory, more channels are introduced until the specification is met.

B. Error Separation

In theory, the channel separation filter $F_i(s)$ can be a causal filter. If $F_i(s)$ is causal, both its phase lag and its passband needs to be considered simultaneously when evaluating (8). This will bring much more troubles into the design. Thus it is preferable that $F_i(s)$ generates no phase shift. The channel filters, $F_i(s)$ with zero-phase characteristics in Fig. 1, can be realized with a Discrete Fourier Transform/Inverse Discrete Fourier Transform (DFT/IDFT) pair or a zero-phase filter.

1) *DFT/IDFT Approach*: Though $F_i(s)$ is considered as continuous, any numerical implementation should use sampled-data. Technical details addressing applying DFT/IDFT as cutoff in ILC were reported in [18]. Fig. 2 demonstrates the error separation into two parts according to two designated frequency bands/channels. Firstly, using DFT, error frequency spectrum $E(j\omega)$ can be obtained from error signal $e(t)$. Secondly, the frequency spectrum $E(j\omega)$ is divided into two designated bands/channels. Thirdly, the rest of the two segments is padded with zero. At last, using IDFT, two error sequences $e1(t)$, $e2(t)$ can be obtained from the two bands of spectrum. This way, the original error signal is separated into two error signals with different frequency spectrums, i.e., $e(t) = e1(t) + e2(t)$.

2) *Zero-Phase Filter Approach*: [18] also discussed the technical issues about using zero-phase filters as cutoff in ILC. A zero-phase filter is not a perfect cutoff device, but rather attenuates the signals above/below the cutoff frequency at a rate determined by the order of the filter. Therefore, two adjacent zero-phase filters will produce an overlapping frequency region between the two designated frequency bands/channels. Fig. 3 demonstrates the partial overlapping between lowpass Filter 1 and highpass Filter 2. ω_{c1} and ω_{c2} are the passband edge frequencies (i.e., cutoff

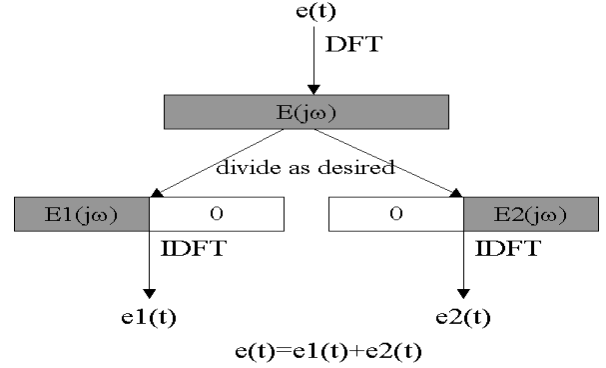


Fig. 2. Error separation via DFT/IDFT

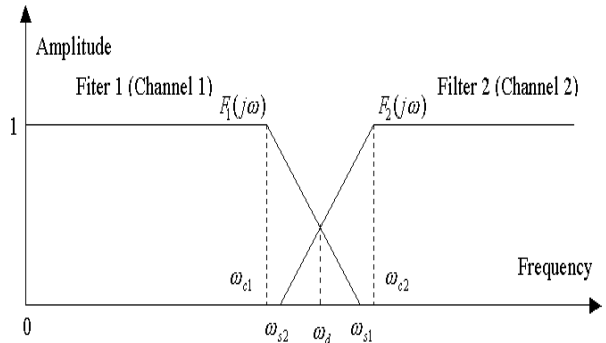


Fig. 3. Frequency overlapping of two filters

frequencies) of Filter 1 and Filter 2, respectively; ω_{s1} and ω_{s2} are the stopband edge frequencies of Filter 1 and Filter 2, respectively [11]. (Note that $\omega_{c1} < \omega_{c2}$ and $\omega_{s2} < \omega_{s1}$). Suppose the overlapping region is $\delta\omega = \omega_{s1} - \omega_{s2}$ and ω_d is the desired separation point of the two designated frequency bands for channels 1 and 2. The equivalent learning compensator inside the region $\delta\omega$, in Laplace form, will be

$$k_1\Phi_1(s)F_1(s) + k_2\Phi_2(s)F_2(s)$$

where $k_1/\Phi_1(s)$ and $k_2/\Phi_2(s)$ are the two learning gains/compensators of channels 1 and 2, respectively. $F_1(s)$ and $F_2(s)$ are the two designated zero-phase filters that define the frequency bands for channels 1 and 2, respectively. Because zero-phase filters generate no phase shift, $F_1(s)$ and $F_2(s)$ are real, positive value functions. Inside the overlapping region, we have $0 < F_1(j\omega) < 1$ and $0 < F_2(j\omega) < 1$, and both learning compensators satisfy the error contraction condition, i.e.,

$$\begin{cases} |1 - k_1G_p(j\omega)\Phi_1(j\omega)| < 1 \\ |1 - k_2G_p(j\omega)\Phi_2(j\omega)| < 1 \end{cases} \quad (11)$$

Then the error contraction rate in the overlapping region $\delta\omega$ is

$$|1 - G_p(j\omega)(k_1\Phi_1(j\omega)F_1(j\omega) + k_2\Phi_2(j\omega)F_2(j\omega))|$$

$$\begin{aligned}
&= |(1 - k_1 G_p(j\omega)\Phi_1(j\omega))F_1(j\omega) + \\
&\quad (1 - k_2 G_p(j\omega)\Phi_2(j\omega))F_2(j\omega) + \\
&\quad 1 - F_1(j\omega) - F_2(j\omega)| \\
&\leq |1 - k_1 G_p(j\omega)\Phi_1(j\omega)|F_1(j\omega) + \\
&\quad |1 - k_2 G_p(j\omega)\Phi_2(j\omega)|F_2(j\omega) + \\
&\quad |1 - F_1(j\omega) - F_2(j\omega)| \\
&< F_1(j\omega) + F_2(j\omega) + |1 - F_1(j\omega) - F_2(j\omega)|.
\end{aligned}$$

If, inside the overlapping region,

$$F_1(j\omega) + F_2(j\omega) < 1 \quad (12)$$

then

$$F_1(j\omega) + F_2(j\omega) + |1 - F_1(j\omega) - F_2(j\omega)| = 1.$$

Thus we have

$$|1 - G_p(j\omega)(k_1\Phi_1(j\omega)F_1(j\omega) + k_2\Phi_2(j\omega)F_2(j\omega))| < 1.$$

Therefore (11) and (12) are the design requirements for the zero-phase filters and learning compensators and these requirements represent sufficient conditions to error contraction in the overlapping region.

Remark 2 After the required individual learning controllers are designed for individual channels, they can be combined into one high order compensator with a common denominator. However, there is no guideline and it is not practical to design this high order compensator directly. The multi-channel method provides the design solution step by step.

IV. APPLICATION TO ANTICIPATORY ILC

The linear anticipatory ILC law [21], [22] has the simple form of

$$u_j(t) = u_{j-1}(t) + k e_{j-1}(t + \Delta) \quad (13)$$

where k is the learning gain and Δ is the lead-time. The error contraction condition (5) for the anticipatory ILC is

$$|1 - k e^{j\Delta\omega} G_p(j\omega)| < 1. \quad (14)$$

Suppose $G_p(j\omega) = N_p(\omega) \exp(j\theta_p(\omega))$ with $N_p(\omega)$ being the magnitude characteristics, and $\theta_p(\omega)$ being the phase characteristics of the system, respectively. From (14), we get

$$\left| 1 - k N_p(\omega) e^{j(\theta_p(\omega) + \Delta\omega)} \right| < 1. \quad (15)$$

This inequality leads to

$$k^2 N_p(\omega) < 2k \cos(\theta_p(\omega) + \Delta\omega). \quad (16)$$

If $k > 0$, we have

$$k N_p(\omega) < 2 \cos(\theta_p(\omega) + \Delta\omega). \quad (17)$$

The frequency range where condition (17) is satisfied is named the *causal range*.

For a minimum phase process

$$G_p(s) = \frac{b_m s^m + b_{m-1} s^{m-1} + \dots + b_1 s + b_0}{s^n + a_{n-1} s^{n-1} + \dots + a_1 s + a_0}$$

with more poles than zeros ($n > m$), the phase characteristics is approaching $-(n-m) \times 90^\circ$. $\theta_p(\omega)$ is bounded while $\Delta\omega$ is approaching $+\infty$. In general, one single channel anticipatory ILC has one constant lead-time and satisfies (17) for a limited frequency band. Using the multi-channel method, we can have the following learning law,

$$u_j(t) = \sum_{i=1}^n u_{i,j}(t) \quad (18)$$

with

$$\begin{cases} u_{1,j}(t) = u_{1,j-1}(t) + k_1 e_{1,j-1}(t + \Delta_1) & \text{In Channel 1} \\ \vdots \\ u_{i,j}(t) = u_{i,j-1}(t) + k_i e_{i,j-1}(t + \Delta_i) & \text{In Channel } i \\ \vdots \\ u_{n,j}(t) = u_{n,j-1}(t) + k_n e_{n,j-1}(t + \Delta_n) & \text{In Channel } n \end{cases} \quad (19)$$

where $e_{i,j-1}$ is the i th error part corresponding to channel i at repetition $(j-1)$. (17) is satisfied in all designated frequency bands/channels with some properly chosen learning gain k_i and lead-time Δ_i ,

$$\begin{cases} k_1 N_p(\omega) < 2 \cos(\theta_p(\omega) + \Delta_1\omega) & \text{In Channel 1} \\ \vdots \\ k_i N_p(\omega) < 2 \cos(\theta_p(\omega) + \Delta_i\omega) & \text{In Channel } i \\ \vdots \\ k_n N_p(\omega) < 2 \cos(\theta_p(\omega) + \Delta_n\omega) & \text{In Channel } n \end{cases} \quad (20)$$

Thus all error components within any of the designated frequency bands/channels will converge to zero in theory. Unlike the self tuning method [14], [23] which uses a repetition switching lead-steps (lead-time), the multi-channel method fixes a lead-time of an anticipatory learning control for each of the designated frequency bands/channels.

V. AN EXAMPLE AND SIMULATIONS

Consider the robot joint example used in [13]:

$$G_p(s) = \frac{8.8}{s + 8.8} \cdot \frac{37^2}{s^2 + 2 \times 0.5 \times 37s + 37^2}.$$

This transfer function is a representation of the closed-loop response of each joint of a RRC robot [5]. It is sufficient complex to exhibit poor transient behavior and has been used for many learning control experiments [5], [6], [12], [13]. Suppose a desired trajectory is given as

$$y_d(t) = 1 - \cos 2\pi t + 0.3(1 - \cos 8\pi t) + 0.2(1 - \cos 38\pi t) + 0.1(1 - \cos 50\pi t) \quad t \in [0, 1] \text{second}$$

and it contains frequency components of 1, 4, 19 and 25 Hz. The integration step size is 0.01s. Learning gain k is fixed as 1 (the reciprocal of DC gain of $G_p(s)$ – the maximum reasonable value suggested by Longman in [12]) in the simulations, i.e. in single channel learning, k is 1 and in multi-channel learning, k is also 1 for all channels. The input of the first trial is $u_0(t) = 0$.

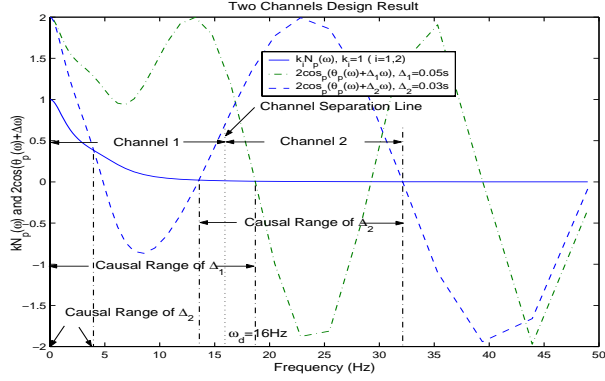


Fig. 4. Two channels' design result

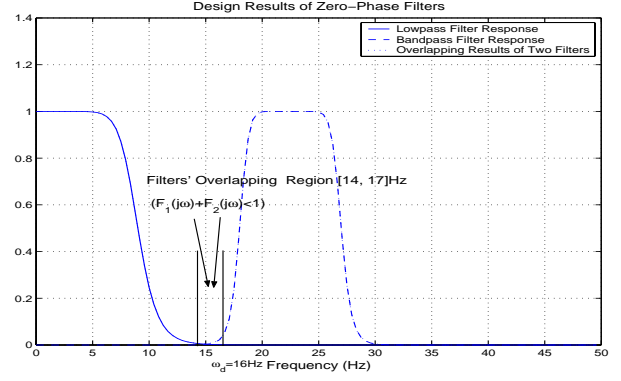


Fig. 5. Design of zero-phase filters

To ensure error convergence of all frequency components, the learning control needs to be adjusted so that (17) is satisfied in a frequency band wider than $[0, 25Hz]$. In the single channel learning, we test a few values of the lead-time Δ (i.e., tune the lead-time Δ) and try to find out a value that can satisfy (17) in the widest frequency range (we plot (17) vs. frequency with different lead-time and find the one that can offer the highest cutoff frequency). Lead-time 0.05second is chosen and it yields a learnable frequency range $[0, 18.7Hz]$. Unfortunately, the components with frequencies 19 and $25Hz$ is not covered. A two-channels learning control is thus employed to extend the maximum learnable frequency from $18.7Hz$ to above $25Hz$. The Δ chosen above in the single anticipatory learning control can be used in channel 1 and renamed as Δ_1 , with values $\Delta_1 = 0.05\text{second}$. To ensure learning of all frequency components, channel 2 must have a designated frequency band to well cover $[18, 25]Hz$. Lead-time $\Delta_2 = 0.03\text{second}$ is chosen and the final design result is shown in Fig. 4. Δ_2 has two causal ranges, $[0, 4]Hz$ and $[13.6, 32]Hz$. The second causal range, $[13.6, 32]Hz$, of Δ_2 overlaps with the causal range, $[0, 18.7]Hz$, of Δ_1 . We can divide $[0, 32Hz]$ into the following two designated bands,

$$\begin{cases} \text{Channel 1 } (0Hz \leq f < 16Hz) & \text{associated with } \Delta_1 \\ \text{Channel 2 } (16Hz \leq f < 32Hz) & \text{associated with } \Delta_2 \end{cases}$$

The channel separation frequency point ω_d , $16Hz$, locates in the middle of $[13.6, 18.7]Hz$ to provide some robustness against the model inaccuracy. When using zero-phase filters to separate the error, the overlapping region of two adjacent filters should locate inside $[13.6, 18.7]Hz$ for the reason of (11) and (12). Then the multi-channel learning law is

$$u_j(t) = u_{1,j}(t) + u_{2,j}(t)$$

with

$$\begin{cases} u_{1,j}(t) = u_{1,j-1}(t) + e_{1,j-1}(t + 0.05) & \text{In Channel 1} \\ u_{2,j}(t) = u_{2,j-1}(t) + e_{2,j-1}(t + 0.03) & \text{In Channel 2} \end{cases}$$

In the single channel learning, lead-time 0.05second is used and the cutoff frequency is set as $18Hz$ (cutoff is

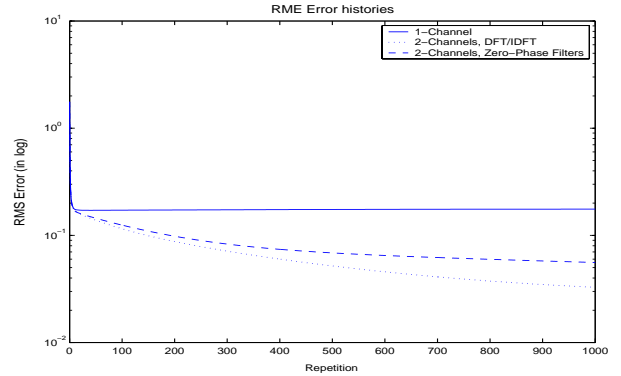


Fig. 6. RMS error histories

realized by DFT/IDFT). In the multi-channel learning, the cutoff frequency is set as $31Hz$. The learnable frequency range of the multi-channel learning control is $[0, 31Hz]$ which is substantially wider than that of the single channel learning control, i.e., $[0, 18Hz]$. Two error separation approaches, the DFT/IDFT approach and the zero-phase filter approach are both tested. For the zero-phase filter approach, a $9Hz$ lowpass 5th order Butterworth filter [25] and a $[18, 27]Hz$ bandpass 10th order Butterworth filter are designed, Fig. 5. Note that (11) and (12) are both satisfied inside the two filters' overlapping region $[14, 17]Hz$ and $[14, 17]Hz$ is $\in [13.6, 18.7]Hz$.

The RMS error histories for the multi-channel learning and the single channel learning are shown in Fig. 6. In the single channel case, the RMS error stops decreasing after about 50 repetitions. Tracking performances of the single channel learning and the multi-channel learning at repetition 1000 are shown in Fig. 6. It is obvious that the multi-channel learning tracks the desired trajectory more accurately than the single channel learning. The simulation results verify the working of the learning controller in channel 2 in the multi-channel case.



Fig. 7. Tracking performances

VI. CONCLUSION

The effectiveness of the frequency characteristics oriented multi-channel method is shown in widening the learnable frequency range. A wider learnable frequency range ensures better tracking performance. The reported experimental results [24] also verified the theory and the proposed design method of this paper. The multi-channel method can also apply to repetitive control. Moreover, because multi-channel learning controller has a few parameters, we can use the auto-tuning idea [14], [23] to tune these parameters, such as lead-time Δ_i , learning gain k_i , and channel separation point ω_d on the fly. The auto-tuning based multi-channel ILC may not need a model.

REFERENCES

- [1] S. Arimoto, S. Kawamura F. and Miyazaki, "Bettering operation of robots by learning," *Journal of Robotic System*, vol. 1, 1984, pp. 123-140.
- [2] N. Amann, D. H. Owens, E. Rogers and A. Wahl, "An H_∞ approach to iterative learning control design," *International Journal of Adaptive Control and Signal Processing*, vol. 10, 1996, pp. 767-781.
- [3] Y.-Q. Chen and K. L. Moore, "On D^α -type iterative learning control," in *Proceedings of the 40th IEEE Conference on Decision and Control*, Orlando, FL, USA, 2001, pp. 4451-4456.
- [4] T.-Y. Doh, K. B. Jin and M. J. Chung, "An LMI approach to iterative learning control for uncertain linear systems," in *proceedings of the 1998 International Symposium on Intelligent and Automatic Control and World Automation Congress*, Anchorage, AK, USA, 1998, pp. ISIAC 006.1-006.6.
- [5] H. Elci, R. W. Longman, M. Phan, J.-N. Juang and R. Ugoletti, "Discrete frequency based learning control for precision motion control," in *Proceedings of the 1994 IEEE International Conference on Systems, Man, and Cybernetics*, San Antonio, TX, USA, 1994, pp. 2767-2773.

- [6] H. Elci, R. W. Longman, M. Phan, J.-N. Juang and R. Ugoletti, "Automated learning control through model updating for precision motion control," *ASME Adaptive Structures and Composite Materials: Analysis and Application*, AD-Vol. 45/MD-Vol. 54, 1994, pp. 299-314.
- [7] C. J. Goh, "A frequency domain analysis of learning control," *Journal of Dynamic Systems, Measurement, and Control*, vol. 116, pp. 781-786, 1994.
- [8] L. M. Hideg and R. P. Judd, "Frequency domain analysis of learning systems," in *Proceedings of the 27th Conference on Decision and Control*, Austin, TX, USA, 1988, pp. 586-591.
- [9] W. Huang and L. Cai, "New hybrid controller for systems with deterministic uncertainties," *IEEE/ASME Transactions on Mechatronics*, vol. 5, 2000, pp. 342-348.
- [10] J.-W. Lee, H.-S. Lee and Z. Bien, "Iterative learning control with feedback using Fourier series with application to robot trajectory tracking," *Robotic*, vol. 11, 1993, pp. 291-298.
- [11] T. Les, *Analog and Digital Filter Design Using C*, Upper Saddle River, NJ: Prentice Hall PTR, 1996.
- [12] R. W. Longman, "Iterative learning control and repetitive control for engineering practice," *International Journal of Control*, vol. 73, no. 10, 2000, pp. 930-954.
- [13] R. W. Longman and T. Songchon, "Trade-offs in designing learning/repetitive controller using zero-phase filter for long term stabilization," *Advances in the Astronautical Sciences*, vol. 102, 1999, pp. 673-692.
- [14] R. W. Longman and S.-L. Wirkander, "Automated tuning concepts for iterative learning and repetitive control laws," in *Proceedings of the 37th IEEE Conference on Decision and Control*, Tampa, FL, USA, 1998, pp. 192-198.
- [15] T. Manabe and F. Miyazaki, "Learning control based on local linearization by using DFT," in *Proceedings of the 1991 IEEE/RSI International Workshop on Intelligent Robots and Systems*, Osaka, Japan, 1991, pp. 639-646.
- [16] J.-H. Moon, T.-Y. Doh and M. J. Chung, "A robust approach to iterative learning control design for uncertain systems," *Automatica*, vol. 34, 1998, pp. 1001-1004.
- [17] M. Phan and J. Juang, "Design of learning controllers based on an auto-regressive representation of a linear system," *AIAA Journal of Guidance, Control and Dynamics*, vol. 19, 1996, pp. 355-362.
- [18] A. M. Plotnik and R. W. Longman, "Subtitles in the use of zero-phase low-pass filtering and cliff filtering in learning control," *Advances in the Astronautical Sciences*, vol. 103, 1999, pp. 673-692.
- [19] A. Tayebi and M. B. Zaremba, "Iterative learning control for non-linear systems described by a blended multiple model representation" *International Journal of control*, vol. 75, 2002, pp. 1376-1383.
- [20] K. K. Tan, H.-F. Dou, Y.-Q. Chen and T. H. Lee, "High precision linear motor control via relay-tuning and iterative learning based on zero-phase filtering," *IEEE Transactions on Control System Technology*, vol. 9, 2001, pp. 244-253.
- [21] D. Wang, "An anticipatory iterative learning control scheme: theory and experiments", in *the Iterative Learning Control Workshop and Roundtable, IEEE CDC'98*, Tampa, FL, USA, 1998, pp. 79-80.
- [22] D. Wang, "On D-type and P-type ILC designs and anticipatory approach," *International Journal of Control*, vol. 73, 2000, pp. 890-901.
- [23] S.-L. Wirkander and R. W. Longman, "Limit cycles for improved performance in self-tuning learning control," *Advances in the Astronautical Sciences*, vol. 102, 1999, pp. 763-781.
- [24] Y. Ye and D. Wang, "Multi-channel design for ILC with robot experiments," in *Proceedings of the 7th International Conference on Control, Automation, Robotics and Vision*, Singapore, 2002, pp. 1066-1070.
- [25] *Signal Processing Toolbox User's Guide*. The Maths Works, Inc., 1997.